Asphaltene Adsorption from Toluene onto Silica Through Thin Water Layers

Xiaozhen Hu[1,3], Maxim P. Yutkin[2], Saleh Hassan[2], Jiangtao Wu[3],
J. M. Prausnitz[1], and C. J. Radke[1,2]

[1] Department of Chemical and Biomolecular Engineering
University of California, Berkeley, USA 94720
[2] Ali I. Al-Naimi Petroleum Engineering Research Center (ANPERC),
Physical Sciences and Engineering Division,
King Abdullah University of Science and Technology (KAUST)
Thuwal, Kingdom of Saudi Arabia 23955-6900
[3] Key Laboratory of Thermo-Fluid Science and Engineering of Ministry of Education,
Xi'an Jiaotong University, Xi'an, China, 710049

Submitted to
Langmuir
November 14, 2018
Revised
November 29, 2018

Corresponding author
Clayton J. Radke
Department of Chemical and Biomolecular Engineering, University of California
101E Gilman Hall
Berkeley, CA 94720-1462
Phone: 510-642-5204
Fax: 510-642-4778
Email: radke@berkeley.edu

Asphaltene Adsorption from Toluene onto Silica Through Thin Water Layers

Xiaozhen Hu[1,3], Maxim P. Yutkin[2], Saleh Hassan[2], Jiangtao Wu[3], J. M. Prausnitz[1], and C. J. Radke[1,2]

[1] Department of Chemical and Biomolecular Engineering
University of California, Berkeley, USA 94720
[2] Ali I. Al-Naimi Petroleum Engineering Research Center (ANPERC),
Physical Sciences and Engineering Division,
King Abdullah University of Science and Technology (KAUST)
Thuwal, Kingdom of Saudi Arabia 23955-6900
[3] Key Laboratory of Thermo-Fluid Science and Engineering of Ministry of Education,
Xi'an Jiaotong University, Xi'an, China, 710049

Abstract

Asphaltenes in crude oil play a pivotal role in reservoir oil production because they control rock-surface wettability. Upon crude-oil invasion into a brine-filled reservoir trap, rock adherence of sticky asphaltene agglomerates formed at the crude oil/brine interface can change the initially water-wet porous medium into mixed-oil wetting. If thick, stable water films coat the rock surfaces, however, asphaltenic-oil adhesion is thought to be prevented. We investigate whether water films influence the uptake of asphaltenes in crude oil onto silica surfaces. Water films of known thickness are formed at a silica surface in a quartz crystal microbalance with dissipation (QCMD) and contacted by toluene-solubilized asphaltene.

We confirm that thick water films prevent asphaltene molecular contact with the silica surface blocking asphaltene adhesion. The thicker the water film, the smaller is the amount of asphaltene deposited. Film thickness necessary for complete blockage onto silica is greater than about 500 nm, well beyond the range of molecular-chain contact. Water films of thickness less than about 500 nm, sandwiched between toluene and solid silica, apparently rupture into thick water pockets and interposed molecularly thin water layers that permit asphaltene adherence.

Introduction

Wettability of oil-reservoir rock is crucial for devising efficient recovery processes.[1] Because oil reservoirs are produced by buoyant oil seeping into previously brine-filled traps, the reservoir rock is initially water-wet. As oil accumulates and water-volume fraction falls, however, many, perhaps all, oil reservoirs shift towards mixed wet where portions of the rock surfaces are oil-wet and portions are water-wet, all within the same local pore space.[2-3] The key to this wettability alteration is the almost universal presence of asphaltenes in crude oil. Asphaltene molecules are defined as soluble in toluene but insoluble in alkanes. They are large sheet-like structures of interconnected heterocyclic rings containing both polar and nonpolar moieties. They are water insoluble and readily aggregate in the oil phase.[4-7] Attachment of asphaltene aggregates to reservoir rock is widely believed to be the origin of mixed wetting.[2, 8] However, because asphaltenes are not soluble in water, they cannot adsorb by reaching the rock surfaces through dissolution into the water phase. Kovscek et al.[2] propose that asphaltene aggregates adsorbed at the oil/brine interface directly deposit or stamp onto rock surfaces when intervening water films rupture during brine expulsion from a developing oil reservoir.

Figure 1 from Freer et al.[9] illustrates the proposed process of asphaltene deposition and wettability alteration. When oil invades a brine-filled rock, water-insoluble asphaltenes in the crude oil congregate irreversibly at the oil/brine interface.[7, 9-11] Rock surfaces are initially protected by thick intervening water layers (Figure 1a). Water-soluble maltenes and resins may leach into the brine phase and adsorb on rock minerals. This adsorption process, however, is apparently not cohesive enough to shift rock wettability significantly. As oil continues to invade, water further drains leaving thin water layers between the rock and oil/brine interfaces. When thin enough, the water films may rupture directly depositing (i.e., stamping) sticky asphaltene moieties onto the rock minerals (Figure 1b). Where water films break, oily asphaltene aggregates coat the rock transforming it to locally oil-wet, primarily at the asperities of exposed surface roughness.[12-13] In rock crevices and corners covered by thick water pockets, however, the rock remains water-wet. This hypothesized scenario produces “mixed-wet” oil reservoirs.[2-3]

The primary supposition underlying mixed-wet oil reservoirs is that water films protect

against asphaltene contact with the rock surfaces and, thus, do not allow oil adhesion.[14-15] To test this supposition, we investigate whether thin water films on a water-wet mineral surface prevent oil-solubilized asphaltenes from depositing. Gonzales and Taylor[16] tackled this problem by exposing quartz powder to air of varying water-vapor relative humidity and then measuring the amount of asphaltene uptake from toluene by concentration depletion. Water film thickness on quartz surfaces for each relative humidity was obtained by Asay and Kim[17] using attenuated total reflection (ATR) – infrared spectroscopy. We also consider asphaltene dissolved in toluene adsorbing through water films onto silica. However, we focus on water films deposited by withdrawing bulk liquid water from a water-wet silica surface placed in a QCMD flow cell, akin to how water drains during from pores during maturation of an oil reservoir. Excellent reviews are available on the application of QCMD to adsorption phenomena.[17A,17B]

Experimental and Methods

Chemicals. Toluene (99.9%, Fisher Chemicals) was used as received to dissolve asphaltene B6 powder kindly provided by Prof. Kilpatrick.[18] Detailed properties of the B6 asphaltene sample are available in Tables 2-5 of Spieker et al.[18] A stock solution of 1 g/L was prepared and stored in a fume hood. Lower concentrations of asphaltene were diluted from the stock solution by adding the desired amount of toluene. Distilled/deionized water was from a MilliQ water system (Synergy®, EMD Millipore Corporation) giving resistivity greater than 18.2 MΩ·cm at 25 ℃.

Apparatus and Procedures. The QCMD instrument was from Biolin Scientific (Model E4, Gothenburg, Sweden). Manufacture-supplied silica-coated quartz sensors (AT-cut, 5 MHz, QXS 303) were used as the adsorbent. Initially, and after each use, silica sensors were cleaned by the following procedure. Sensors were first rinsed with MilliQ water followed by blow-drying with nitrogen. The sensors were then placed in an air-plasma cleaner (Harrick Plasma Cleaner, 110V, PDC-32G, medium intensity) for 10 min. AFM (Bruker Dimension Icon Model, Bruker Corporation, Massachusetts, CA, USA) was used to evaluate the resulting rms surface

roughness of selective initially cleaned silica sensors under air tapping mode at approximately 1 nm in agreement with literature.[18A] After cleaning, the sensors were immediately transferred into the flow module (QFM 401) of the QCMD instument and aligned to the desired position. To ensure repeatability, each sensor was normally used for no more than 5 times. An exception was for those experiments with asphaltene irreversibly adsorbed onto dry silica where pristine sensors were used. Temperature was set constant at 25 ℃.A temperature equilibration of 30 to 60 min was allowed before initiating flow experiments.

For asphaltene adsorption studies onto dry silica, pure toluene was first injected into the QCMD flow cell by a peristaltic pump (ISMATEC, ISM935C) installed with 2-Stop Viton tubing (0.64 mm I.D., Cole-Parmer) at 100 μL/min. Resonant frequency and dissipation kinetics of the first, third, fifth, seventh, and ninth overtones were recorded simultaneously. Flushing was continuous for about 1 to 2 h until a stable baseline was achieved defined by a frequency shift of each overtone of less than 0.2 Hz per hour. Asphaltene adsorption was then measured by injecting a sequence of increasing concentrations of asphaltene dissolved in toluene from 1 mg/L to 1000 mg/L. After each concentration increase, toluene flushing was performed to test for possible desorption.

For asphaltene uptake measurement out of toluene through an intervening water layer, a stable air baseline was first achieved. MilliQ water was then pumped for 30 to 40 min. Next, water films were formed above the sensor surface by connecting the flow-cell outlet to a laboratory vacuum supply, allowing slow removal of bulk liquid water and replacement with ambient air. Depending on vacuum duration, water layers of various thickness were obtained. Details of water-film formation are described below. Pure toluene was injected following water-layer deposition. Next, an asphaltene-in-toluene solution (15 mg/L, water-saturated toluene) flowed into the QCMD cell. Finally, at the end of each flow experiment, excess toluene was flushed through the entire system. The cell was disassembled and the sensor cleaned as described above.

QCMD Theory. To interpret the observed QCMD frequency and dissipation signals, we adopt the continuum-mechanics framework of Voinova et al.[19] Figure 2 displays the case of a

homogeneous thin water film of thickness h_L covered by a second semi-infinite immiscible fluid, e.g., oil or air. Both the water layer and the covering fluid are Newtonian, incompressible and contain no adsorbing species. Continuum momentum balances are written for the thin liquid layer and for the immiscible overlayer fluid and coupled through no-slip and stress-continuity boundary conditions. Once expressions for the velocity profiles are established, the friction force by the thin liquid layer on the oscillating crystal, F_f, divided by the velocity amplitude of the crystal, V_o, is calculated to evaluate a beta factor: $\beta \equiv F_f / V_o$.[19] We find that

$$\beta = \eta_L k_L (1+i) \frac{1 - Ae^{2k_L h_L (1+i)}}{1 + Ae^{2k_L h_L (1+i)}}, \tag{1}$$

where

$$A = \frac{1 + \eta k / \eta_L k_L}{1 - \eta k / \eta_L k_L}, \tag{2}$$

ρ_L and η_L are density and viscosity of the water layer, and ρ and η are density and viscosity of the bulk overlayer fluid, respectively. k_L and k in Eq. 2 are wave numbers or inverse characteristic decay lengths of the thin water layer and the bulk covering fluid defined, respectively, by $k_L = \sqrt{\rho_L \omega / 2\eta_L}$ and $k = \sqrt{\rho\omega / 2\eta}$. $\omega = 2\pi n f^*$ is angular frequency with f^* the fundamental resonant crystal frequency in air or vacuum (4.95 MHz), and n is the overtone number (1, 3, 5, etc.). Eq. 2 differs algebraically from that of Voinova et al.[19] (compare Eq. 11 of that manuscript). In the case of air as the covering immiscible fluid, $A = 1$.

Given the beta factor, predicted frequency and dissipation shifts in QCMD follow from Eq. 15 of Voinova et al.[19] In the two-fluid case of Eqs. 1 and 2, we find that

$$\frac{\Delta f_n}{n} = \frac{\eta_L k_L}{2\pi n \rho_q h_q} \frac{1 - A^2 e^{4h_L k_L} - 2Ae^{2h_L k_L} \sin 2h_L k_L}{1 + A^2 e^{4h_L k_L} + 2Ae^{2h_L k_L} \cos 2h_L k_L}, \tag{3}$$

and

$$\Delta D_n = -\frac{\eta_L k_L}{\pi n f^* \rho_q h_q} \frac{1 - A^2 e^{4h_L k_L} + 2Ae^{2h_L k_L} \sin 2h_L k_L}{1 + A^2 e^{4h_L k_L} + 2Ae^{2h_L k_L} \cos 2h_L k_L}, \tag{4}$$

where h_q is the thickness of the quartz crystal (0.334 mm) and ρ_q is its mass density (2648 kg/m^3).

Eqs. 3 and 4 are not restricted to thin water layers. Beyond a thickness of $3/k_L \sim 750$ nm, the water-layer thickness is effectively infinite. Eqs. 3 and 4 simplify to

$$\frac{\Delta f_n}{n} = -\frac{\eta_L k_L}{2\pi n \rho_q h_q} = -\frac{1}{n^{1/2}} \frac{\sqrt{f^*/\pi}}{2\rho_q h_q} \sqrt{\rho_L \eta_L}\,, \tag{5}$$

and

$$\Delta D_n = \frac{\eta_L k_L}{\pi n f^* \rho_q h_q} = \frac{1}{n^{1/2} \rho_q h_q \sqrt{\pi f^*}} \sqrt{\rho_L \eta_L}\,. \tag{6}$$

Frequency shifts are negative, whereas dissipation shifts are positive. Properties of the covering fluid no longer contribute at large water-film thickness. Eqs. 5 and 6 thus apply to any fluid-filled cell (with no solute adsorption).

For thin water films where $h_L k_L \ll 1$, Eqs. 3 and 4 reduce to

$$\frac{\Delta f_n}{n} = -\frac{f^* \rho_L h_L}{\rho_q h_q}\left[1 - \frac{\rho\eta}{\rho_L \eta_L}\right] - \frac{1}{n^{1/2}} \frac{\sqrt{f^*/\pi}}{2\rho_q h_q} \sqrt{\rho\eta} + O(h_L k_L)^2\,, \tag{7}$$

and

$$\Delta D_n = \frac{1}{n^{1/2} \rho_q h_q \sqrt{\pi f^*}} \sqrt{\rho\eta} + O(h_L k_L)^2\,. \tag{8}$$

To order thickness squared, only the viscous properties of the covering layer contribute to dissipation. The frequency shift for thin water layers, however, is influenced both by the mass of the water layer (i.e., $\rho_L h_L$) and by the overlayer fluid properties.

Figure 3 shows frequency shift from Eq. 3 as a function of water-layer thickness when the covering overlayer is air (i.e., $\rho\eta = 0$) for two overtone numbers 1 and 5. We rely on the 5th overtone experimentally because it is typically more precise. For large water-layer thicknesses, the frequency shift approaches that of a bulk water layer in Eq. 5. Water layers beyond a thickness of about 500 nm are equivalent to a QCMD cell filled with water. At small film thicknesses, a linear-decline regime appears in agreement with Eq. 7. Similar results for dissipation are obtained from Eq. 4 and highlighted in Figure 4. In accord with Eq. 8, asymptotic approach to zero thickness is now quadratic, rather than linear in Figure 3.

We study the role a thin water layer on the adsorption of asphaltene from crude oil solubilized in a toluene overlayer. As justified later, the adsorbed asphaltene layer is approximated as homogeneous and rigid. For dilute asphaltene concentrations that do not influence toluene viscosity and density, continuum theory is a simple extension of Eq. 3:

$$\frac{\Delta f_n}{n} = -\frac{f^*\hat{\Gamma}}{\rho_q h_q} + \frac{\eta_L k_L}{2\pi n \rho_q h_q} \frac{1 - A^2 e^{4h_L k_L} - 2Ae^{2h_L k_L} \sin 2h_L k_L}{1 + A^2 e^{4h_L k_L} + 2Ae^{2h_L k_L} \cos 2h_L k_L}, \tag{9}$$

or of Eq. 7 for a thin water film

$$\frac{\Delta f_n}{n} = -\frac{f^*\hat{\Gamma}}{\rho_q h_q} - \frac{f^*\rho_L h_L}{\rho_q h_q}\left[1 - \frac{\rho\eta}{\rho_L \eta_L}\right] - \frac{1}{n^{1/2}} \frac{\sqrt{f^*/\pi}}{2\rho_q h_q} \sqrt{\rho\eta} + O(h_L k_L)^2, \tag{10}$$

where $\hat{\Gamma}$ is the toluene-dissolved asphaltene-solute mass uptake per unit area. The inverse of the instrument constant multiplying solute adsorption in Eqs. 9 or 10 equals 17.7 ng/(cm^2 Hz) for a 5-MHz AT-cut quartz crystal and is commonly given the symbol *C*. The first term in Eq. 10 is the classical result of Sauerbrey.[20] Dissipation in Eq. 4 or Eq. 8 for a thin intervening water layer is unchanged upon asphaltene adsorption because a rigid (or purely elastic) adsorbed layer suffers no viscous loss.

Eqs. 3-10 are relative to a baseline of the crystal oscillating in air (or vacuum). With other baseline choices, theory for that baseline is subtracted from theory appropriate for the measured frequency and dissipation kinetics.

Deposition of Thin Water Films. To deposit a thin water film of known thickness between the silica surface and the toluene oil phase, we rely on the water-wetting properties of the QCMD flow cell. Water tends to reside adjacent to the silica surface in the flow cell completely displacing non-wetting toluene. Conversely, toluene does not completely displace water in a cell but leaves a water film adjacent to the silica surface.[21-22] Figure 5 confirms this behavior. Initially, in Figure 5, toluene is flushed through the cell giving a zero baseline signal. Pure water is then injected for 30 min causing frequency to fall and dissipation to rise sharply. Dashed lines show the theoretical predictions from Eqs. 5 and 6 for a water-filled cell relative to a toluene-filled cell baseline. Excellent agreement is found using known viscosities and densities of water and toluene. Thus, water completely displaces immiscible toluene from the

flow cell containing a silica floor. After about 40 min of water injection, toluene is again flushed. No change occurs in either frequency or dissipation. The explanation is that a thick water layer beyond 500 nm remains adjacent to the silica surface that appears infinite to the oscillating crystal. This observation allows us to deposit water films on the silica surface of varying thickness and then inject toluene without displacing the intervening water layer.

To establish the initial water-film thickness, we open the flow inlet and apply a slight vacuum to the flow outlet of an initially water-filled QCMD cell. During this process, we observe frequency and dissipation kinetics. By stopping water withdrawal at various times, finite-thickness water films remain on the silica surface.

Figure 6 illustrates the film-deposition process. At 12 min, water fills the empty cell. Frequency declines and dissipation increases obeying theory in Eqs. 5 and 6, as shown by dashed lines. Water withdrawal in curve 2 starts at 80 min and lasts until about 100 min when withdrawal stops. At that time, frequency and dissipation stabilize. Theory in Eq. 3 (with A=1) specifies a water-layer thickness near 16 nm. Similar results hold for curves 1 and 3 with curve 1 representing essentially dry silica ($h_L \sim 0$) and curve 3 representing a thick water film ($h_L >$ 500). Different water-film thicknesses are achieved by choosing different withdrawal-stoppage times.

Results and Discussion

Asphaltene Adsorption from Toluene on Dry Silica. Figure 7 gives the 5th overtone frequency ($\Delta f_5/5$, black) and dissipation (ΔD_5, red) kinetics relative to pure toluene for asphaltene adsorption and desorption from toluene on a dry silica surface. Each increase in asphaltene concentration leads to an additional step decline in frequency. Dissipation only slightly increases consonant with a rigid or elastic adlayer. These two markers signify asphaltene adsorption according to the Sauerbrey term of Eq. 9 (or 10). Density-viscosity correction for the asphaltene-toluene solution is negligible; we assume no change in the water-layer thickness upon asphaltene adsorption. Zero dissipation change is consistent with negligible viscosity-density change and with a rigid adsorbed layer. The higher the asphaltene concentration, the larger is the adsorption amount ascertained from the Sauerbrey term in Eq.

10 relative to the toluene baseline.

Figure 8 graphs asphaltene adsorption, $\hat{\Gamma}$ (mg/m^2), as a function of concentration in toluene after 30 min of exposure time. Black squares represent the experimental data. The solid line is calculated from the Langmuir expression[23]:

$$\hat{\Gamma} = \frac{\hat{\Gamma}_{\max} Kc}{1 + Kc} \tag{11}$$

where c is asphaltene concentration (mg/L), $\hat{\Gamma}_{max}$ is maximum adsorption (9.7 mg/m^2) and K is the Langmuir equilibrium constant (0.17 L/mg). Our measured amounts are in general agreement with literature despite differences in asphaltene sources.[24-29] Asphaltene strongly adsorbs from toluene onto silica when not in the presence of water.

Following each increase in asphaltene concentration in Figure 7, but before the next increase, pure toluene was injected to desorb asphaltene (denoted by vertical arrows). There is only a small frequency increase after each ~ 25-min toluene flush. Most all the adsorbed asphaltene on dry silica is irreversibly bound. Thus, asphaltene adsorption from toluene onto dry silica is both strong and mostly irreversible. This conclusion is consistent with available literature.[24-30] Agreement with the Langmuir equilibrium model in Figure 7 is incompatible because of the observed irreversible attachment of toluene-solubilized asphaltene to the silica surface. However, slow rearrangement kinetics of initially reversible adsorbed configurations can lead to an early-time apparent Langmuir isotherm.[31-32]

Asphaltene Adsorption from Toluene through an Intervening Water Layer. Figure 9 shows an example of frequency-dissipation kinetics for the injection sequence: water baseline, water-film deposition, pure toluene, loading of 15 mg/L asphaltene in toluene, and final toluene flush. The rise of frequency and fall in dissipation upon withdrawal of liquid water from the QCMD cell at 10 min corresponds to the formation of a thin water layer in air. At 30 min, pure toluene is injected. Frequency declines and dissipation increases corresponding to replacing inviscid air in the cell by viscous toluene. Flushing of toluene for 50 min causes little change in signals indicating that the water-layer thickness remains unchanged. At 80 min, a 15 mg/L asphaltene-toluene solution is injected with frequency falling and dissipation unchanging. We

attribute this result to uptake of asphaltene from toluene onto the silica surface in the presence of the thin water layer. Finally, at 120 min, pure toluene is flushed with both frequency and dissipation remaining constant. We interpret this result as irreversible asphaltene adsorption.

With A=1, Eq. 3 (minus baseline correction from Eq. 5) and Eq. 4 (minus baseline correction from Eq. 6) specify a water-film thicknesses in Figure 9 of 47 nm from frequency (labeled 1) and 110 nm from dissipation (labeled 2), respectively. Upon toluene injection at 30 min, theory in Eq. 3 with A = 1 minus Eq. 3 evaluated at A from Eq. 2 gives a thickness from frequency of 37 nm (labeled 3) while Eq. 6 with A = 1 minus Eq. 6 evaluated at A from Eq. 2 gives a water-film thickness of 99 nm (labeled 4). The frequency decline after injection of the 15 mg/L asphaltene solution is interpreted as asphaltene uptake (labeled 5) and quantified by the Sauerbrey expression as $\hat{\Gamma} = 1.5\ \mathrm{mg/m^2}$. Subsequent toluene flushing maintains this surface density.

The experiment in Figure 9 was repeated for several different deposited water-layer thicknesses. Results are shown as filled squares in Figure 10, along with results (filled circles) from Gonzales and Taylor[16] for water films deposited onto silica by molecular vapor adsorption from humidified air. Our measurements from liquid water-film deposition concur with those of Gonzales and Taylor[16]: thicker water layers reduce asphaltene uptake. Even though specific asphaltene samples are different, uptake amounts are similar. However, we find that sorption reduction apparently requires thicker films than do Gonzales and Taylor.[16] Water films larger than ~ 500 nm completely protect against asphaltene deposition. A thick water layer physically separates insoluble asphaltene molecules from the silica/water surface. In all cases, we find that when asphaltene attachment through water layers occurs, it is essentially irreversible.

Asphaltene molecules solubilized in oil do not dissolve into a surrounding water phase and adsorb onto a water-enveloped mineral surface. Rather asphaltene moieties at the oil/water interface molecularly deposit onto the solid surface when the protective water film breaks.[9, 14-15] Our results in Figure 10 confirm that water layers protect against asphaltene deposition. Although the trend in Figure 10 of decreasing asphaltene sorption with increasing water-film thickness is consistent with that of Gonzales and Taylor,[16] the striking difference is that we

record substantially thicker films. The films of Gonzales and Taylor[16] are molecular up to a few nm thickness. However, we detect much thicker films necessary to reduce asphaltene uptake. Direct contact of asphaltene-aggregate side-chain moieties dangling from an oil/water interface to a mineral surface demands molecularly thin intervening water films. An explanation for our contrary observation in Figure 10 emanates from Figure 1b. Thin water films sandwiched between an asphaltene-laden oil phase and a wetting solid surface are not likely homogeneous even for flat solid surfaces. Film rupture leaves behind trapped water microdroplets that average in a QCMD experiment to a thicker film than that ruptured between the microdroplets.[9] Asphaltene surface-attachment amounts in Figure 10 thus correspond to an average of drop-covered regions and regions between the microdrops where water layers are molecularly thin. We suggest that our thicker water films correspond to more leave-behind water patches. Consequently, the 500-nm water-film thickness for complete protection against asphaltene deposition in Figure 10 reflects a stable water film. Beyond this thickness, wetting water films remain intact to protect against asphaltene attachment. Smaller thicknesses, however, breakup allowing molecular asphaltene contact with the silica surface between microdrops.[9] We suggest that the discrepancies found in Figure 9 between film thicknesses calculated from frequency and from dissipation also arise from inhomogeneous water films.

The observations of Gonzales and Taylor[16] likely provide a more realistic estimate of water-layer thicknesses that prevent direct contact of oil/brine-interface asphaltene moieties to a solid surface (i.e., around a few Angstroms). However, in reservoir application, water films deposit through a water-drainage process, not through molecular vapor adsorption. Inhomogeneous, ruptured water films are expected during drainage. Thus, thicker water films than those obtained by Gonzales and Taylor[16] are required to prevent asphaltene attachment to sandstone reservoir surfaces. Although our study focuses on pure water films, aqueous brine films are expected to behave similarly.

Conclusions

Asphaltene molecules and aggregates dissolved in crude oil play an overarching role in the behavior of oil reservoirs. Once attached to rock surfaces, asphaltene aggregates can

produce local oil-wet regions that redistribute oil and water phases in the pore spaces. In this work, we form liquid-water films between silica and asphaltene-laden toluene by a drainage process in a QCMD flow cell. Continuum theory assesses the film thicknesses and the surface densities of attached asphaltene. We confirm the hypothesis that thick water films prevent attachment of asphaltene to a water-wet silica-mineral surface. In a drainage process, rupture of water films is prerequisite for the adhesion of asphaltene to a mineral surface. When protective water films rupture, attachment of asphaltene moieties to silica is irreversible. Water thicknesses required to prevent asphaltene deposition correspond to film stability. Once water films rupture, molecularly thin water layers apparently emerge that allow direct molecular contact of asphaltene to a mineral surface.

Author Information

Corresponding Author
Clayton J. Radke
Email: radke@berkeley.edu

Notes

The authors declare no competing financial interest.

Acknowledgments

Xiaozhen Hu gratefully acknowledges the China Scholarship Council (CSC) and the National Natural Science Foundation of China (No. 51476130) for financial assistance during his stay at the University of California, Berkeley. Saleh Hassan was supported by the Ali I. Al-Naimi Petroleum Research Center (ANPERC) at the King Abdullah University of Science and Technology (KAUST), Thuwal, KSA.

References

1. Morrow, N. R., Wettability and Its Effect on Oil Recovery. *Journal of Petroleum Technology* **1990,** *42* (12), 1476-1484.
2. Kovscek, A. R.; Wong, H.; Radke, C. J., A pore-level scenario for the development of mixed wettability in oil reservoirs. *AIChE Journal* **1993,** *39* (6), 1072-1085.
3. Salathiel, R. A., Oil Recovery by Surface Film Drainage In Mixed-Wettability Rocks. *Journal of Petroleum Technology* **1973,** *25* (10), 1216-1224.
4. Sjöblom, J.; Simon, S.; Xu, Z., Model molecules mimicking asphaltenes. *Advances in Colloid and Interface Science* **2015,** *218*, 1-16.
5. Adams, J. J., Asphaltene Adsorption, a Literature Review. *Energy & Fuels* **2014,** *28* (5), 2831-2856.
6. Mullins, O. C.; Sabbah, H.; Eyssautier, J.; Pomerantz, A. E.; Barre, L.; Andrews, A. B.; Ruiz-Morales, Y.; Mostowfi, F.; McFarlane, R.; Goual, L.; Lepkowicz, R.; Cooper, T.; Orbulescu, J.; Leblanc, R. M.; Edwards, J.; Zare, R. N., Advances in Asphaltene Science and the Yen-Mullins Model. *Energy & Fuels* **2012,** *26* (7), 3986-4003.
7. Langevin, D.; Argillier, J. F., Interfacial behavior of asphaltenes. *Advances in Colloid and Interface Science* **2016,** *233*, 83-93.
8. Buckley, J. S.; Takamura, K.; Morrow, N. R., Influence of Electrical Surface Charges on the Wetting Properties of Crude Oils. *SPE Reservoir Engineering* **1989,** *4* (03), 332-340.
9. Freer, E. M.; Svitova, T.; Radke, C. J., The role of interfacial rheology in reservoir mixed wettability. *Journal of Petroleum Science and Engineering* **2003,** *39* (1-2), 137-158.
10. Jeribi, M.; Almir-Assad, B.; Langevin, D.; Hénaut, I.; Argillier, J. F., Adsorption Kinetics of Asphaltenes at Liquid Interfaces. *Journal of Colloid and Interface Science* **2002,** *256* (2), 268-272.
11. Cagna, A.; Esposito, G.; Quinquis, A.-S.; Langevin, D., On the reversibility of asphaltene adsorption at oil-water interfaces. *Colloids and Surfaces A: Physicochemical and Engineering Aspects* **2018,** *548* (548), 46-53.
12. Brady, P. V.; Morrow, N. R.; Fogden, A.; Deniz, V.; Loahardjo, N.; Winoto, Electrostatics and the Low Salinity Effect in Sandstone Reservoirs. *Energy & Fuels* **2015,** *29* (2), 666-677.
13. Schmatz, J.; Urai, J. L.; Berg, S.; Ott, H., Nanoscale imaging of pore-scale fluid-fluid-solid contacts in sandstone. *Geophysical Research Letters* **2015,** *42* (7), 2189-2195.
14. Buckley, J. S.; Morrow, N. R., Characterization of Crude Oil Wetting Behavior by Adhesion Tests. In *SPE/DOE Enhanced Oil Recovery Symposium*, Tulsa, Oklahoma, 1990.
15. Buckley, J. S., Evaluation of Reservoir Wettability and its Effect on Oil Recovery. *US DOE Report* **1999,** *DE-FC22-96ID13421*.
16. Gonzalez, V.; Taylor, S. E., Asphaltene adsorption on quartz sand in the presence of pre-adsorbed water. *Journal of Colloid and Interface Science* **2016,** *480*, 137-145.
17. Asay, D. B.; Kim, S. H., Evolution of the Adsorbed Water Layer Structure on Silicon Oxide at Room Temperature. *The Journal of Physical Chemistry B* **2005,** *109* (35), 16760-16763.
17A. Reviakine, I.; Johannsmann,D.; Richter, R. P., Interpreting Quartz Crystal Microbalance Data from Solvated Interfaces. *Analytical Chemistry* **2011**, *83*, 8838-8848.

17B. Johannsmann, D., *The Quartz Crystal Microbalance in Soft Matter Research: Fundamentals and Modeling,* Springer, New York, 2014.
18. Spiecker, P. M.; Gawrys, K. L.; Kilpatrick, P. K., Aggregation and solubility behavior of asphaltenes and their subfractions. *Journal of Colloid and Interface Science* **2003,** *267* (1), 178-193.
18A. Wang, L.; Siretanu, I.; Duits, M. H. G.; Stuart, M. A. C.; Mugele, F., Ion effects in the adsorption of carboxylate on oxide surfaces, studied with quartz crystal microbalance. *Colloids and Surfaces A: Physicochemical and Engineering Aspects* **2016,** *494*, 30-38.
19. Voinova, M. V.; Rodahl, M.; Jonson, M.; Kasemo, B., Viscoelastic acoustic response of layered polymer films at fluid-solid interfaces: Continuum mechanics approach. *Phys Scripta* **1999,** *59* (5), 391-396.
20. Sauerbrey, G., Verwendung von Schwingquarzen zur Wägung dünner Schichten und zur Mikrowägung. *Zeitschrift für Physik* **1959,** *155* (2), 206-222.
21. Bretherton, F. P., The motion of long bubbles in tubes. *Journal of Fluid Mechanics* **1961,** *10* (02), 166. XX need final page
22. Erzuah, S.; Fjelde, I.; Voke Omekeh, A., Wettability Estimation by Oil Adsorption Using Quartz Crystal Microbalance with Dissipation QCM-D. In *SPE Europec featured at 80th EAGE Conference and Exhibition*, Society of Petroleum Engineers: Copenhagen, Denmark, 2018.
23. Berg, J. C., *An Introduction to Interfaces & Colloids: The Bridge to Nanoscience*. World Scientific: Singapore, 2010.
24. Ekholm, P.; Blomberg, E.; Claesson, P.; Auflem, I. H.; Sjöblom, J.; Kornfeldt, A., A Quartz Crystal Microbalance Study of the Adsorption of Asphaltenes and Resins onto a Hydrophilic Surface. *Journal of Colloid and Interface Science* **2002,** *247* (2), 342-350.
25. Dudáa ová, D.; Silset, A.; Sjöblom, J., Quartz Crystal Microbalance Monitoring of Asphaltene Adsorption/Deposition. *Journal of Dispersion Science and Technology* **2008,** *29* (1), 139 - 146.
26. Farooq, U.; Sjöblom, J.; Øye, G., Desorption of Asphaltenes from Silica-Coated Quartz Crystal Surfaces in Low Saline Aqueous Solutions. *Journal of Dispersion Science and Technology* **2011,** *32* (10), 1388 - 1395.
27. Keleşoğlu, S.; Volden, S.; Kes, M. r. i.; Sjöblom, J., Adsorption of Naphthenic Acids onto Mineral Surfaces Studied by Quartz Crystal Microbalance with Dissipation Monitoring (QCM-D). *Energy & Fuels* **2012,** *26* (8), 5060-5068.
28. Abudu, A.; Goual, L., Adsorption of Crude Oil on Surfaces Using Quartz Crystal Microbalance with Dissipation (QCM-D) under Flow Conditions. *Energy & Fuels* **2009,** *23* (3), 1237-1248.
29. Hannisdal, A.; Ese, M.-H.; Hemmingsen, P. V.; Sjöblom, J., Particle-stabilized emulsions: Effect of heavy crude oil components pre-adsorbed onto stabilizing solids. *Colloids and Surfaces A: Physicochemical and Engineering Aspects* **2006,** *276* (1-3), 45-58.
30. Yang, G.; Chen, T.; Zhao, J.; Yu, D.; Liu, F.; Wang, D.; Fan, M.; Chen, W.; Zhang, J.; Yang, H.; Wang, J., Desorption Mechanism of Asphaltenes in the Presence of Electrolyte and the Extended Derjaguin Landau Verwey Overbeek Theory. *Energy & Fuels* **2015,** *29* (7), 4272-4280.

31. Maurer, S. A.; Bedbrook, C. N.; Radke, C. J., Competitive Sorption Kinetics of Inhibited Endo- and Exoglucanases on a Model Cellulose Substrate. *Langmuir* **2012,** *28* (41), 14598-14608.
32. Cascão Pereira, L. G.; Hickel, A.; Radke, C. J.; Blanch, H. W., A kinetic model for enzyme interfacial activity and stability: pa-hydroxynitrile lyase at the diisopropyl ether/water interface. *Biotechnology and Bioengineering* **2002,** *78* (6), 595-605.

Figures

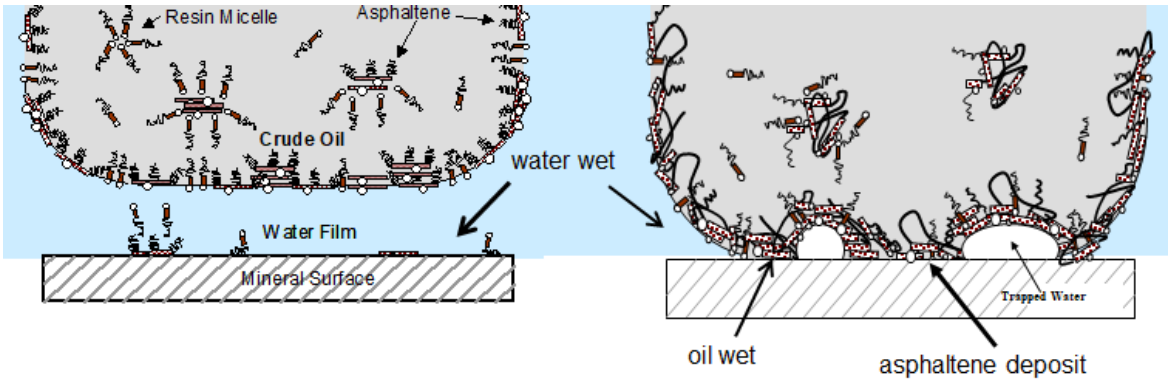

Figure 1. Stamping of asphaltene agglomerates (skins) formed at the crude-oil/brine interface. (a) Onto mineral surfaces upon rupture of protective water films (b). Rupture process leaves patches of brine on the surface. After Freer et al.[9] with permission.

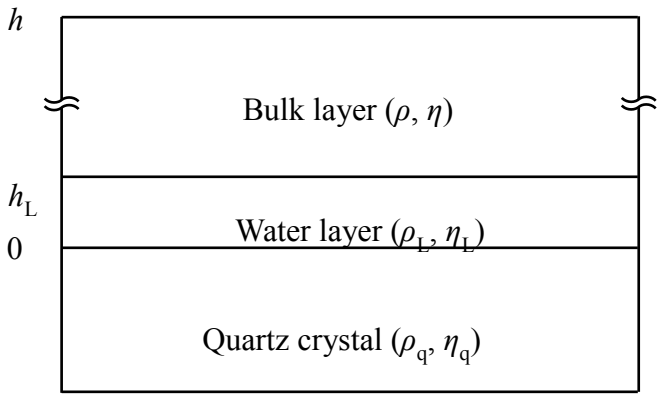

Figure 2. Schematic of QCMD crystal covered by a thin water layer of thickness h_L, immersed in a covering fluid of semi-infinite thickness. Densities and viscosities of each compartment are labeled by ρ and η, respectively.

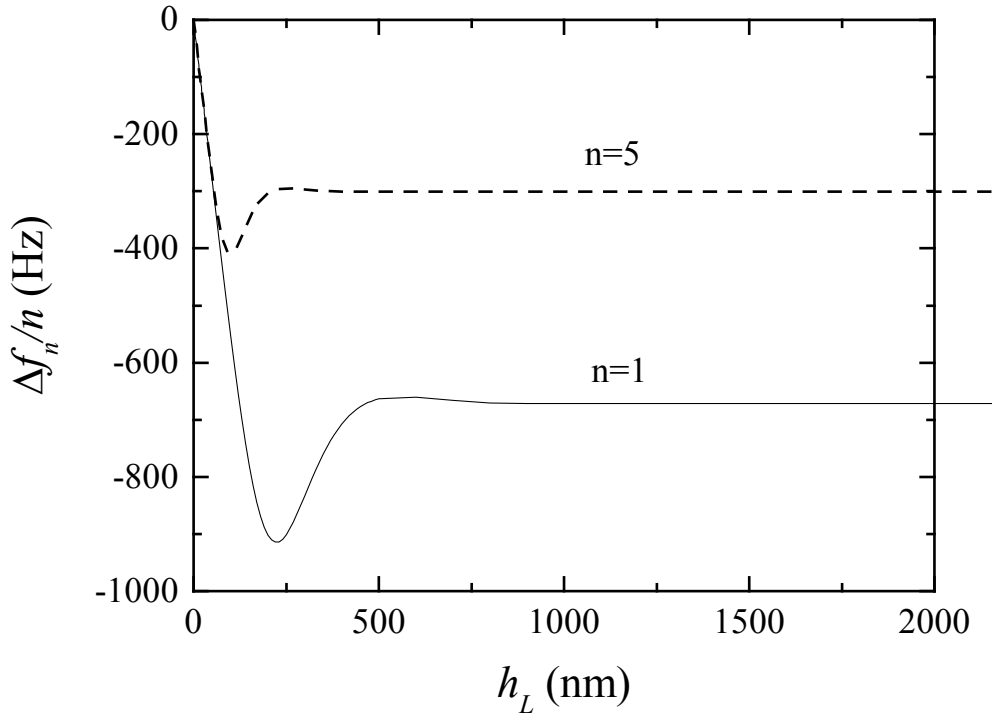

Figure 3. Predicted frequency change for a water film covered by air as a function of layer thickness h_L. First and fifth frequency overtones are calculated from Eq. 3.

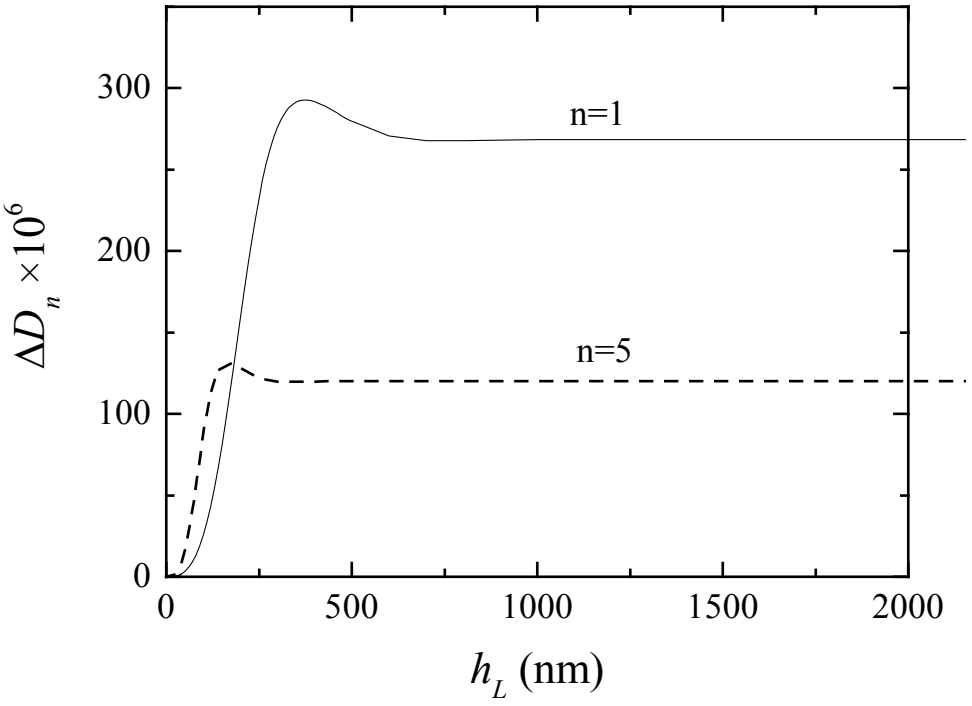

Figure 4. Predicted dissipation change for a water film covered by air as a function of layer thickness h_L. First and fifth frequency overtones are calculated from Eq. 4.

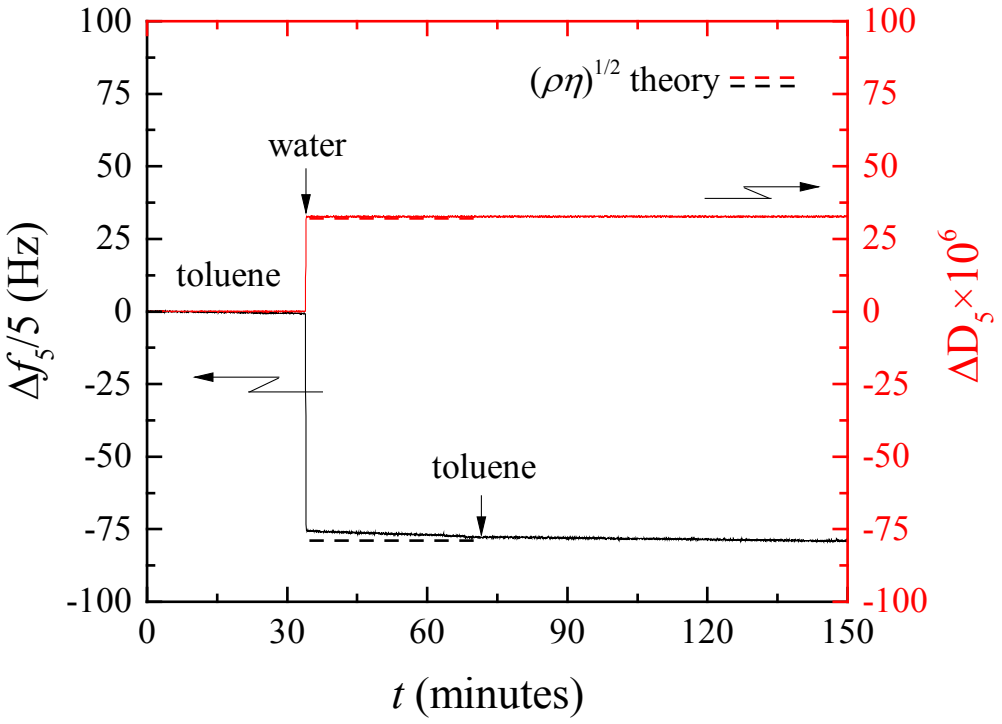

Figure 5. Frequency (black) and dissipation (red) kinetics (5th overtone) relative to toluene baseline for the injection sequence toluene, water, and toluene.

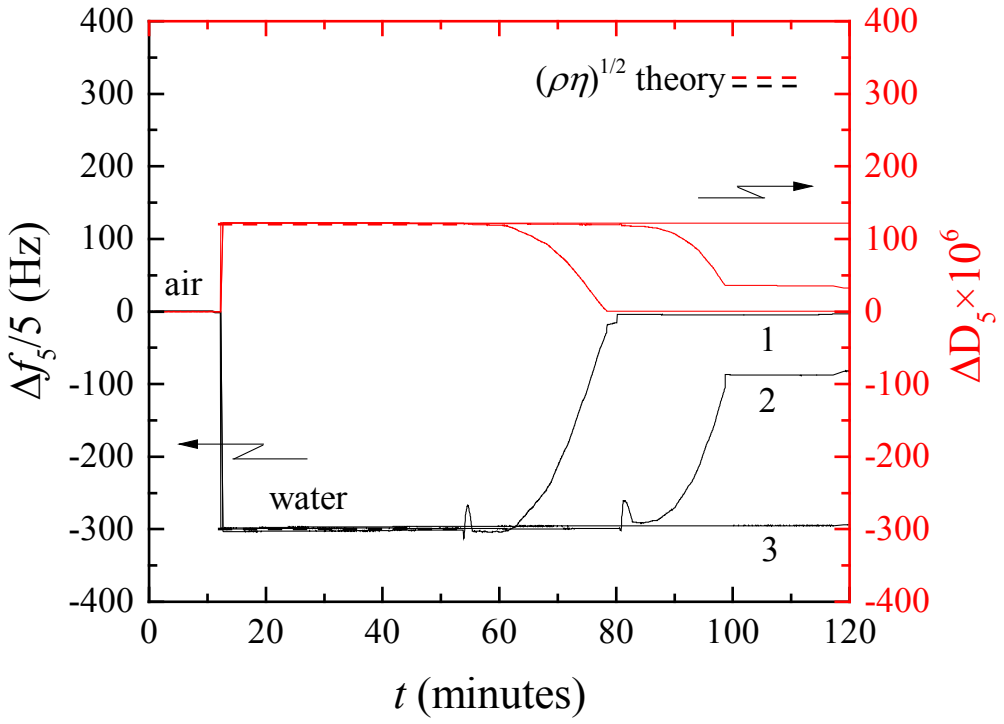

Figure 6. Frequency (black) and dissipation (red) kinetics (5th overtone) relative to air baseline for three water-withdrawal stoppages after (1) 30 min; (2) 20 min; and (3) no withdrawal stoppage. Curve 1 corresponds to essentially dry silica (without water layer). Curve 2 exhibits a thin water layer ~ 16 nm, and curve 3 corresponds to silica covered by a thick, bulk water. Spikes correspond to initiation of water withdrawal.

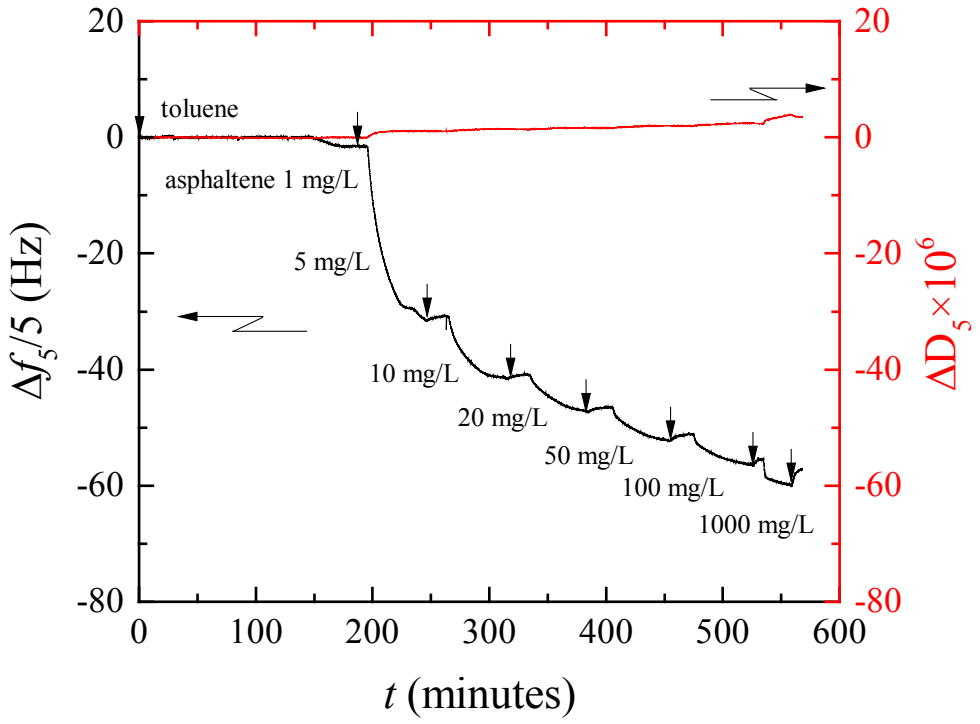

Figure 7. Sequence of frequency (black) and dissipation (red) kinetics (5th overtone) for asphaltene adsorption from toluene on dry silica. Each injection step corresponds to increasing asphaltene concentration. Vertical arrows indicate injection of pure toluene before the subsequent higher asphaltene concentration.

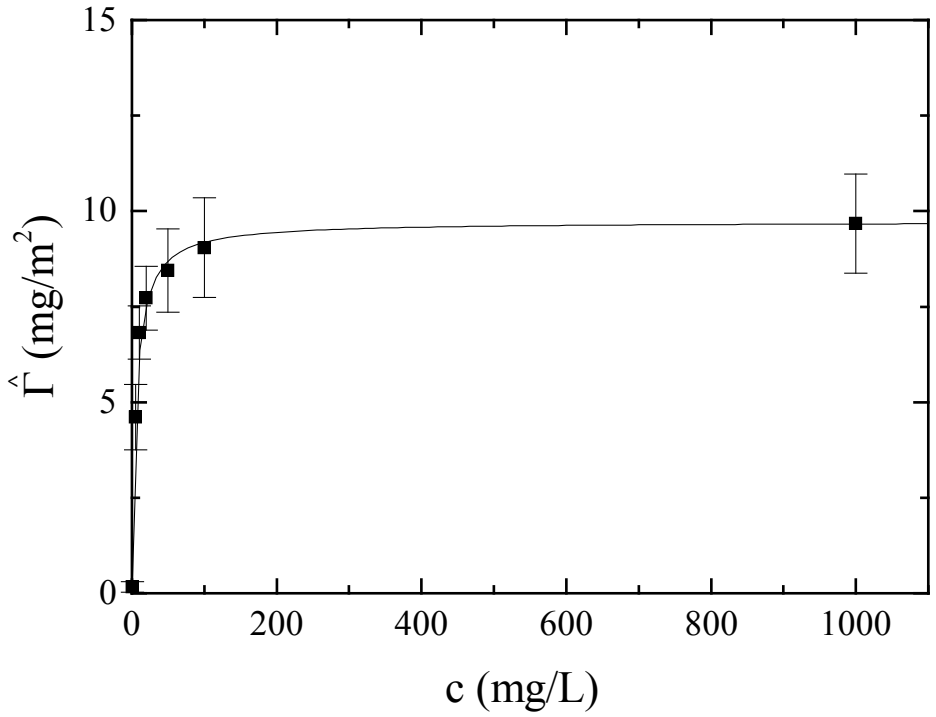

Figure 8. Asphaltene adsorption from toluene onto dry silica after 30 min exposure as a function of concentration (filled squares). The solid line corresponds to the Langmuir equation with $\hat{\Gamma}_{max}$ = 9.7 mg/m^2 and K = 0.17 L/mg. Typical error bar corresponds to measurement repeatability.

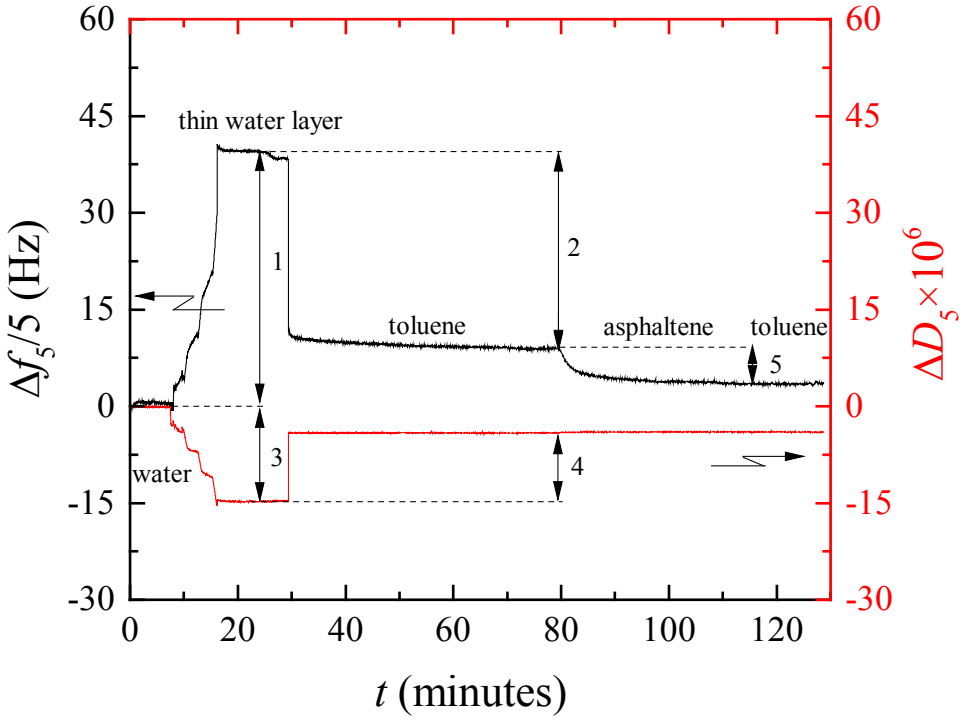

Figure 9. Frequency (black) and dissipation (red) kinetics (5th overtone) for asphaltene adsorption from water-saturated toluene onto silica through a thin water layer. Injection sequence is: water baseline, water withdrawal, toluene, asphaltene in toluene (15 mg/L), and toluene flush. Thicknesses are from theory applied to the labeled frequency and dissipation differences: (1) h_L ~ 47 nm; (2) h_L ~37 nm; (3) h_L ~ 110 nm; (4) h_L ~ 99 nm; and (5) $\hat{\Gamma} \sim 1.5$ mg/m^2.

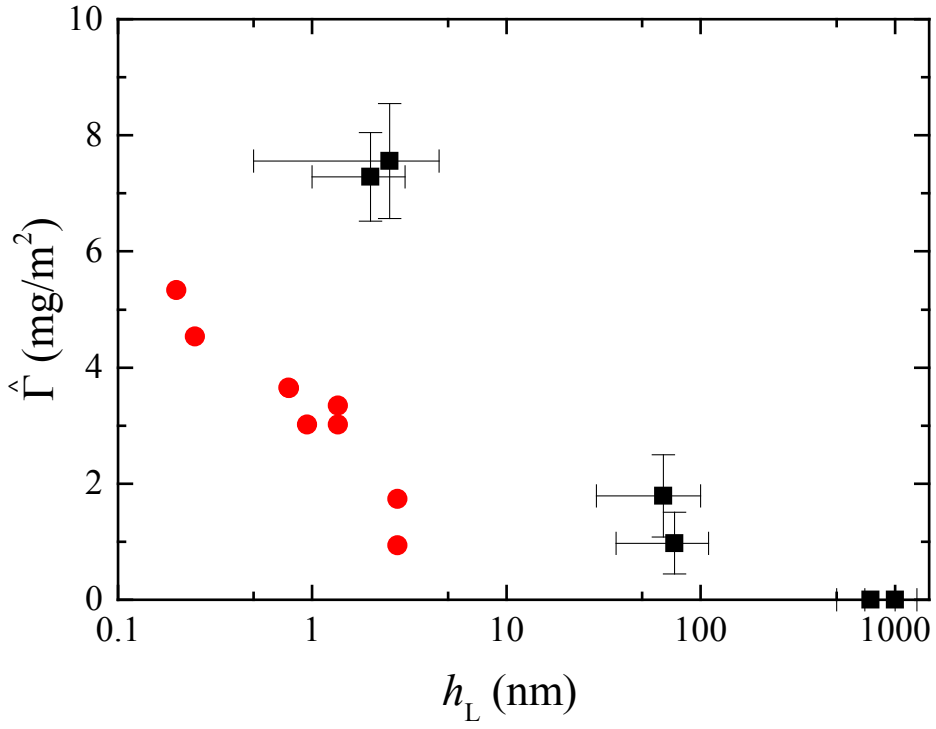

Figure 10. The influence of water thickness h_L on asphaltene adsorption from toluene amount (filled squares). Filled circles are from Gonzalez and Taylor.[16] Asphaltene concentration is 15 mg/L.

Table of Contents Graphic